Complete Description of the Xe 4*d* Photoionization by Spin-Resolved Photoelectron and Auger Spectroscopy

G. Snell,[1,2] B. Langer,[2,3] M. Drescher,[1] N. Müller,[1] B. Zimmermann,[2]
U. Hergenhahn,[2] J. Viefhaus,[2] U. Heinzmann,[1] and U. Becker[2]
[1]*Fakultät für Physik, Universität Bielefeld, Universitätsstraße 25, D-33615 Bielefeld, Germany*
[2]*Fritz-Haber-Institut der Max-Planck-Gesellschaft, Faradayweg 4-6, D-14195 Berlin, Germany*
[3]*Max-Born-Institut für Nichtlineare Optik und Kurzzeitspektroskopie, Rudower Chaussee 6, D-12489 Berlin, Germany*
(Received 26 August 1998)

Spin-resolved photoelectron and Auger spectra were measured near the maximum of the Xe 4*d* photoionization at 93.8 eV. The results were used to derive a complete set of relativistic dipole matrix elements and their relative phases. These transition amplitudes are compared with theoretical calculations and a semiempirical approach utilizing a critical survey of the present experimental photoionization data. This analysis shows that this prominent photoionization process may be well described within a 4-parameter model. [S0031-9007(99)08746-3]

PACS numbers: 32.80.Hd, 32.80.Fb

Photoionization of the xenon 4*d* subshell is a showcase example for atomic inner-shell photoionization similar to helium for outer-shell double excitation. This is because the photoionization of this subshell exhibits strong electron correlation effects [1–3] in addition to pronounced single particle phenomena [4] such as shape resonances and Cooper minima [5,6] which makes it difficult to distinguish between the different origins for a certain behavior of the partial cross section, as well as other photoionization properties. This is why numerous studies of the Xe 4*d* photoionization were performed during the last decade regarding the partial cross section σ and angular distribution anisotropy parameter β [7]. However, concerning a complete description of the Xe 4*d* photoionization in terms of matrix elements and their relative phases only very few experimental studies exist [8,9].

The first of these studies was photoelectron Auger coincidence experiments [8] which caused a controversy about the magnitude of the phase shift between two partial waves with the same angular momentum l but different total angular momentum j [10]. A critical evolution of the data and later experiments [11] pointed to a very small phase shift; however, the corresponding error bars were still high. Another open question refers to the total number of photoionization parameters really necessary for a complete description of the Xe 4*d* photoionization. In a strict relativistic approach ten parameters would be necessary: three partial waves $\varepsilon(l, j)$ and two relative phases Δ_j for each spin-orbit component $4d_{3/2}$ and $4d_{5/2}$ of the final ionic state [12]. On the other extreme assuming LS coupling only two partial waves $\varepsilon(l + 1)$ and $\varepsilon(l - 1)$ would govern the 4*d* photoionization in xenon, which means including their relative phase shift Δ_l three parameters altogether [13,14]. The relatively large experimental uncertainties of the former coincidence experiments did not allow us to draw definite conclusions concerning this point. Therefore, further experiments with complementary methods such as measuring the spin polarization of the emitted electrons should be performed in order to solve this problem.

We have carried out such spin-resolved experiments for the Xe 4*d* photolines and subsequently emitted $N_{4,5}O_{2,3}O_{2,3}$ Auger lines at $h\nu = 93.8$ eV. In this way we were able to measure as many independent photoionization parameters as necessary for a complete relativistic treatment in addition to the already known quantities σ and β. The analysis of the measured data within this approach showed a surprising result: the relativistic phases became nearly zero but again with a relatively large uncertainty due to an extremely sensitive dependence of this phase upon the different spin polarization parameters. However, setting this phase exactly zero results in a consistent set of matrix elements and remaining phases with very low error bars. Further analysis of the data assuming LS coupling showed that two partial wave amplitudes R_p and R_f and one phase shift Δ_{pf} are indeed sufficient to describe the Xe 4*d* photoionization if instead of the statistical ratio for the intensities of the spin-orbit components one uses the corresponding experimental ratios or relativistic calculations [15]. That means that four independent photoionization parameters are sufficient to completely describe the Xe 4*d* photoionization within a few percent of accuracy. This result is corroborated by a semiempirical approach using measured σ, β, and alignment values A_{20} published during the last few years for a large range of photon energies [7].

The experiments were performed at the synchrotron radiation facilities HASYLAB at DESY (Hamburg) and BESSY (Berlin) using the undulator beam lines BW3 and U1, respectively. The delivered photons were employed to ionize an effusive beam of xenon atoms. Both beam lines were constructed to produce highly linearly polarized radiation. Using a multilayer acting as a quarter-wave plate [16] we were able to convert this into circularly polarized light. Thus we could determine both kinds of spin polarization of the electrons: P_{trans} the transferred

 0031-9007/99/82(12)/2480(4)$15.00

polarization from circularly polarized light to the emitted electron and P_{dyn} the so-called dynamical polarization being connected with an excitation by linearly polarized light [17]. The electron spin polarization was measured using a spherical Mott detector in combination with a time-of-flight electron spectrometer which has been employed recently for the spin polarization measurements of photoelectrons and Auger electrons emitted during Xe $3d$ photoionization [18]. The main advantage for this new instrument compared to more conventional Mott polarimeters is the fact that all photoelectrons and Auger lines in a spectrum are counted simultaneously. The detected electrons were emitted under 90° respectively, 70° with respect to the incoming light at an angle of 135° with respect to the plane defined by the linear polarization and the propagation direction.

Figure 1 shows a measured spectrum for the Xe $4d$ photolines along with the spin polarization of the two spin-orbit components underneath. The polarization sensitivity S_{eff} of the Mott polarimeter was determined to be 0.20(3) by measuring the Xe $5p_{1/2}$ photolines which are completely described by three photoionization parameters only in any approach. The spin polarizations of associated pairs of photoelectron and Auger lines show opposite signs due to the singlet coupling of the doubly charged final ionic states depicted here.

Concerning theory the results are in very good agreement with the relativistic random phase approximation (RRPA) calculations of Johnson and Cheng [10,19]. Figure 2 shows the derived reduced dipole matrix elements and relative phases [20] in comparison with other measured and calculated data. Considering the good agreement between theory and experiment at one photon energy the question arises how well we are able to describe the photon energy dependence of the different photoionization parameters from the present set of data. For this purpose we have analyzed the data situation for all photoionization parameters which have been measured over larger energy ranges; these are partial cross section σ, angular distribution asymmetry, and alignment parameters β and A_{20}.

This critical analysis was done considering two points: first, the existence of more recent and more precise data and, second, the examination of relations between the different photoionization parameters which restrict the values of the different parameters to stay within certain limits [21]. The most obvious example for such a relationship is exhibited in the case of a Cooper minimum due to one vanishing partial wave, here the f wave. In this case all photoionization parameters are fixed numbers, e.g., the angular distribution parameter β becomes 0.2 and the alignment parameter $A_{20} = -0.748$ which is the most negative value allowed [15]. Because there is a Cooper minimum in the partial cross section around 180 eV the β value of 0.2 is an additional indicator for the exact position of the Cooper minimum, determining in turn the alignment value to be -0.748 at this energy. The best curve derived from the sequence of published β values crosses the value of 0.2 at 176 eV fixing the corresponding minimum in the alignment curve.

Figures 3(a)–3(d) show critically selected measured data for σ, spin-orbit branching ratio ρ, β, and A_{20} along with semiempirical and calculated curves. Our semiempirical analysis based on consistency checks for all parameters in a certain energy region yields β values

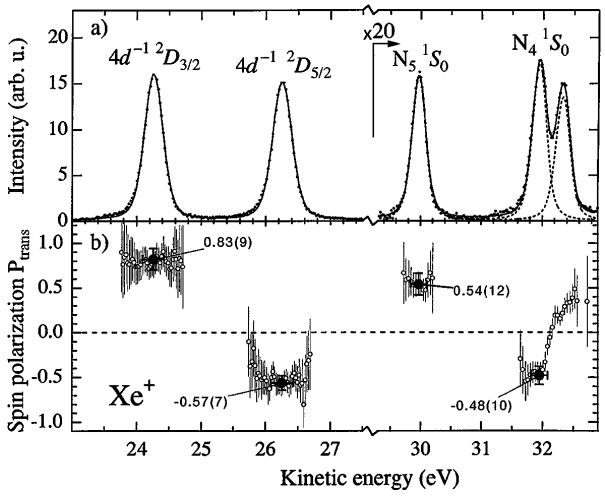

FIG. 1. Xe $4d$ electron spectrum at $h\nu = 93.8$ eV (a) along with the degree of spin polarization of the two spin-orbit components underneath (b). Detection geometry as described in the text.

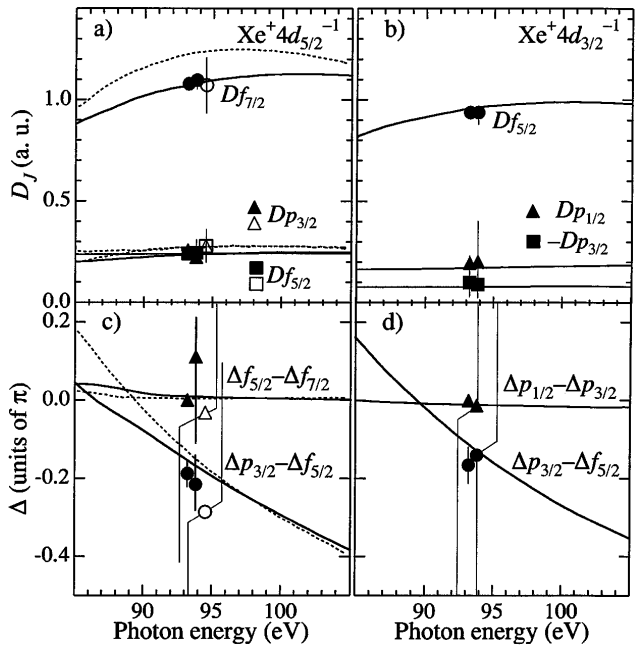

FIG. 2. Comparison between experimentally determined reduced dipole matrix elements shown in length form (a),(b) and relative phases (c),(d) with calculations using a completly relativistic approach (RRPA). Closed symbols (data with smaller error bars are the result from a restricted analysis with a fixed relativistic phase of zero) represent data from this work, the open symbols are from [8], the solid lines are from [10], and the dotted lines are from [19].

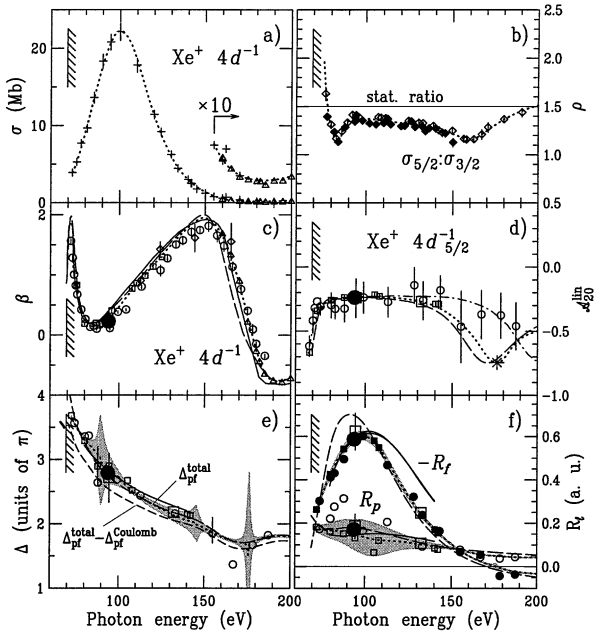

FIG. 3. Xe $4d$ partial cross section σ (a), spin-orbit branching ratio ρ (b), angular distribution anisotropy β parameter (c), and alignment values A_{20} (d) are shown with the derived dipole matrix elements (f) for the partial εp and εf wave photoelectron emission and their relative phase shift (e) [15]. Measured data are taken from (a) [22] (+) and [23] (△); (b) [24] (◆) and [25] (◇); (c) [26] (◇), [27] (○), [23] (△), and [28] (□); (d) [27] (○) and [28] (□); the star points to the best A_{20} value compatible with the corresponding β value. The dotted lines and small open circles (e) and filled circles (f) represent a semiempirical analysis. The dipole matrix elements and phases (large ●, □) are derived from higher differential measurements [8,9] and the alignment values calculated in turn from these values (large ●, □) are shown in (d). The dash-dotted curves in (d) represent HF calculations [4,29]. The solid curve in (c) is a RRPA calculation [30], whereas these curves in (e) and (f) show RRPA calculations [19] and the dashed lines are RPA results [31]. In (e) the short line below threshold represents our HF quantum defect calculation [32].

slightly above those of Ref. [27]. The same analysis has been applied with respect to the alignment A_{20} with the additional requirement that the minimal A_{20} should occur at 176 eV. The semiempirical curves derived from such a procedure are basically consistent with a 3-parameter approach if one considers the sum of the Xe $4d_{3/2}$ and Xe $4d_{5/2}$ partial cross section, besides β and A_{20}, only. The partitioning into the spin-orbit components has to be taken into account separately, which means that this quantity is treated as another independent parameter so that we are practically dealing with a 4-parameter model. The deeper reason for the validity of this model is the approximate jk-coupling of the photoelectron and the ionic core, which means that the photoelectron is governed basically by LS coupling, whereas the spin-orbit branching ratio of the final ionic state is influenced by relativistic effects [33]. The semiempirical curves make it possible to derive semiempirical matrix elements and their relative phase shift.

The result is shown in Figs. 3(e) and 3(f). We note that at certain energies the error bars of the semiempirically derived data become very large, as depicted by the shaded areas. These are the energies where additional, more highly differential measurements, such as the ones reported here, are necessary to perform. These data points are particularly useful to determine the semiempirical phase shift at the most critical energies, e.g., near Cooper minima [34]. Having these points fixed the vast rest of the energy dependent phase shift behavior can be determined very reliably from each set of good quality data of at least three independent photoionization parameters, in most cases σ, β, and A_{20}.

In order to derive also accurate partial cross sections the measured spin-orbit branching has to be taken into account explicitly, which means that a set of four parameters is sufficient to reproduce all other photoionization parameters within a few percent of accuracy (see Fig. 4) if the phase shift at the critical energies is determined by additional independent measurements. Comparing our result with the different theoretical approaches reveals another surprising result. The calculated curves, relativistic [10] and nonrelativistic [31] ones, are very close to each other and to the semiempirical curves except for the f-wave radial matrix elements. For the latter the relativistic calculation including relaxation fits the low energy part of the f-wave contribution very well where it overestimates this contribution at higher energies. On the contrary the nonrelativistic calculation without relaxation describes the high energy part very well, whereas it overshoots the empirical values at lower energies. Combining both calculations for the appropriate energy range gives a very good description of the overall behavior. This means, however, that the main problem of theory at present is to a lesser extent the

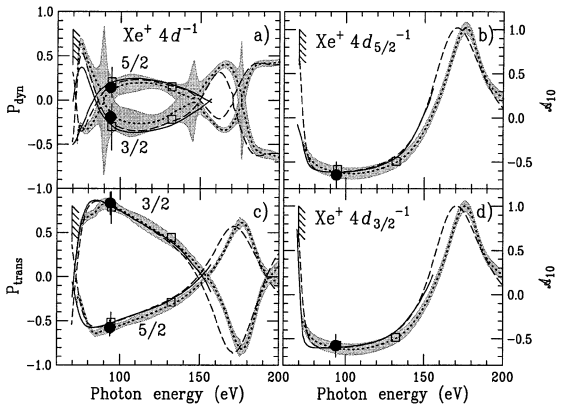

FIG. 4. Dynamical (a) and transferred (c) spin polarization of Xe $4d$ photoelectrons (emitted under 90° with respect to the incoming light and having 135° with respect to the electric field vector for linearly polarized light) along with the orientation parameters A_{10} of the remaining ions with $4d_{5/2}$ (b) and $4d_{3/2}$ (d) holes [17]. Our measured values are shown by closed circles, whereas the experimentally derived data [8,9] are given by open squares. The solid curves represent RRPA calculations [19], the dashed curve represents RPA calculation [31], and the dotted lines represent the semiempirical values.

phase dependent dynamical part rather than the relaxation problem. This is, in fact, an old and well-known problem [35] but nevertheless still not being solved in a satisfactory fashion. An energy dependent treatment of the relaxation seems to be necessary in order to overcome this problem. Despite this particular drawback theory is capable of describing the photoionization of the Xe $4d$ subshell, in particular, their dynamics, surprisingly well.

In summary, we have performed the first spin-resolved measurements of the photoelectrons and Auger electrons resulting from photoionization of the Xe $4d$ subshell. This measurement made it possible to analyze the $4d$ photoionization in terms of dipole matrix elements and relevant phases regarding the quantum mechanically complete description of this process. The surprising result of this analysis is the fact that Xe $4d$ photoionization outside of Cooper minima may be described within a relatively simple model which requires two partial waves with one phase shift only if one takes the measured spin-orbit branching ratio into account.

This work was supported in part by the Deutsche Forschungsgemeinschaft. The support of T. Möller and F. Schäfers is gratefully acknowledged.

[1] M. Y. Amusia *et al.*, Sov. Phys. JETP **39**, 752 (1974).
[2] J. B. West *et al.*, J. Phys. B **9**, 407 (1976).
[3] M. Y. Amusia and M. Kutzner, *VUV- and Soft X-Ray Photoionization*, edited by U. Becker and D. A. Shirley (Plenum Press, New York, 1996).
[4] D. J. Kennedy and S. T. Manson, Phys. Rev. A **5**, 227 (1972).
[5] J. W. Cooper, Phys. Rev. Lett. **13**, 762 (1964).
[6] J. W. Cooper, Phys. Rev. **128**, 681 (1962).
[7] U. Becker and D. A. Shirley, in *VUV- and Soft X-Ray Photoionization* (Ref. [3]).
[8] B. Kämmerling and V. Schmidt, Phys. Rev. Lett. **67**, 1848 (1991).
[9] S. J. Schaphorst *et al.*, J. Phys. B **30**, 4003 (1997).
[10] W. R. Johnson and K. T. Cheng, Phys. Rev. Lett. **69**, 1144 (1992).
[11] B. Kämmerling and V. Schmidt, Phys. Rev. Lett. **69**, 1145 (1992); J. Phys. B **26**, 1141 (1993).
[12] K.-N. Huang, W. R. Johnson, and K. T. Cheng, At. Data Nucl. Data Tables **26**, 33 (1981).
[13] J. Cooper and R. N. Zare, J. Chem. Phys. **48**, 942 (1968).
[14] N. A. Cherepkov, J. Phys. B **13**, L689 (1980).
[15] The relations between σ, β, A_{20}, ρ, R_p, R_f, and Δ_{pf} are $\sigma = \frac{4}{3}\pi^2 \times \alpha \times h\nu \times 2(2R_p^2 + 3R_f^2)$, where $h\nu$ is the photon energy in hartree, $\alpha \approx 1/137$, and R_l are given in atomic units $a_0/\sqrt{\text{hartree}}$ with a_0 being the Bohr radius,
$$\rho = \sigma_{5/2}/\sigma_{3/2},$$
$$\beta = (2R_p^2 + 12R_f^2 - 36R_pR_f\cos\Delta_{pf})/(10R_p^2 + 15R_f^2),$$
$$A_{20}^{5/2} = -\sqrt{\frac{8}{7}}\,\frac{7R_p^2+3R_f^2}{10R_p^2+15R_f^2}, \qquad A_{20}^{3/2} = -\frac{7R_p^2+3R_f^2}{10R_p^2+15R_f^2}.$$
[16] J. Viefhaus *et al.*, Phys. Rev. Lett. **77**, 3975 (1996).
[17] The relations between P_{trans}, P_{dyn}, A_{10}, ρ, R_p, R_f, and Δ_{pf} are expressed as
$$P_{\text{trans}}^{5/2} = \frac{1}{\rho+1}\,\frac{10R_p^2-15R_f^2-5R_pR_f\cos\Delta_{pf}}{7R_p^2+12R_f^2-6R_pR_f\cos\Delta_{pf}} = -\frac{1}{\rho}P_{\text{trans}}^{3/2},$$
$$P_{\text{dyn}}^{5/2} = \frac{1}{\rho+1}\,\frac{-25R_pR_f\sin\Delta_{pf}}{7R_p^2+12R_f^2-6R_pR_f\cos\Delta_{pf}} = -\frac{1}{\rho}P_{\text{dyn}}^{3/2},$$
$$A_{10}^{5/2} = \sqrt{\frac{7}{15}}\,\frac{3R_p^2-3R_f^2}{2R_p^2+3R_f^2}, \qquad A_{10}^{3/2} = \sqrt{\frac{9}{20}}\,\frac{3R_p^2-3R_f^2}{2R_p^2+3R_f^2}.$$
[18] G. Snell *et al.*, Phys. Rev. Lett. **76**, 3923 (1996).
[19] W. R. Johnson and K. T. Cheng, Phys. Rev. A **46**, 2952 (1992).
[20] These matrix elements are related to their LS independent matrix elements and the branching ratio ρ by
$$d_{3/2}^{-1}\text{:}\ R_f = -\sqrt{\frac{\rho+1}{6}}\,D_{f_{5/2}},$$
$$R_p = -\sqrt{\frac{6(\rho+1)}{4}}\,D_{p_{3/2}} = \sqrt{\frac{6(\rho+1)}{20}}\,D_{p_{1/2}},$$
$$\Delta p_{1/2} - \Delta p_{3/2} = 0, \qquad \Delta p_{3/2} - \Delta f_{5/2} = \Delta_{pf} + \pi,$$
$$d_{5/2}^{-1}\text{:}\ R_f = -\sqrt{\frac{21(\rho+1)}{6\rho}}\,D_{f_{5/2}} = -\sqrt{\frac{21(\rho+1)}{120\rho}}\,D_{f_{7/2}},$$
$$R_p = \sqrt{\frac{\rho+1}{4\rho}}\,D_{p_{3/2}},$$
$$\Delta p_{3/2} - \Delta f_{5/2} = \Delta_{pf} + \pi, \qquad \Delta f_{5/2} - \Delta f_{7/2} = 0.$$
[21] K. N. Huang, Phys. Rev. A **22**, 223 (1980).
[22] U. Becker *et al.*, Phys. Rev. A **39**, 3902 (1989).
[23] D. W. Lindle *et al.*, Phys. Rev. A **37**, 3808 (1988).
[24] B. W. Yates *et al.*, Phys. Rev. A **31**, 1529 (1985).
[25] A. Ausmees *et al.*, Phys. Rev. A **51**, 855 (1995).
[26] L. Torop, J. Morton, and J. B. West, J. Phys. B **9**, 2035 (1976).
[27] S. Southworth *et al.*, Phys. Rev. A **28**, 261 (1983).
[28] B. Kämmerling, Inaugural thesis, Universität Freiburg, 1991 (unpublished).
[29] E. G. Berezhko, N. M. Kabachnik, and V. S. Rostovsky, J. Phys. B **11**, 1749 (1978).
[30] M. Kutzner, V. Radojevic, and H. P. Kelly, Phys. Rev. A **40**, 5052 (1989).
[31] N. A. Cherepkov, J. Phys. B **12**, 1279 (1979).
[32] R. D. Cowan, *The Theory of Atomic Structure and Spectra* (University of California Press, Berkeley, 1981).
[33] U. Becker, J. Electron Spectrosc. Relat. Phenom. **96**, 105 (1998).
[34] U. Heinzmann and N. A. Cherepkov, in *VUV- and Soft X-Ray Photoionization* (Ref. [3]).
[35] Z. Altun, M. Kutzner, and H. P. Kelly, Phys. Rev. A **37**, 4671 (1988).